1994

Flash Pyrolysis-Gas Chromatography/Mass Spectrometry of Lower Kittanning Vitrinites: Changes in the Distributions of Polyaromatic Hydrocarbons as a Function of Coal Rank

Michael A. Kruge
Montclair State University, krugem@mail.montclair.edu

David F. Bensley
Southern Illinois University Carbondale

PREPRINT: Kruge, M.A. and Bensley, D.F., 1994, Flash pyrolysis-gas chromatography/ mass spectrometry of Lower Kittanning vitrinites: Changes in the distributions of polyaromatic hydrocarbons as a function of coal rank. In, Mukhophadyay, P. K. and Dow, W.G., eds., *Vitrinite Reflectance as a Maturity Parameter: Applications and Limitations*. American Chemical Society Symposium Series 570, p. 136-148.
DOI: 10.1021/bk-1994-0570.ch009. ISBN: 9780841229945

Flash Pyrolysis-Gas Chromatography/Mass Spectrometry of Lower Kittanning Vitrinites: Changes in the Distributions of Polyaromatic Hydrocarbons as a Function of Coal Rank

Michael A. Kruge and David F. Bensley

Department of Geology, Southern Illinois University
Carbondale, IL 62901, USA

Abstract: Chemical analyses restricted to a single coal maceral permit a focus on rank effects without concern for variations in organic matter type. Vitrinite concentrates of high purity were isolated from coal samples of the Lower Kittanning seam by multi-step density gradient centrifugation, with reflectances ranging from 0.66 to 1.39% R_{max}. In addition to the previously recognized losses of phenolic compounds, the vitrinite pyrolyzates exhibit marked increases in relative concentrations of tri- and tetraaromatic hydrocarbons (especially benzo[*a*]fluorene, methyl-phenanthrenes, methylfluorenes and methylchrysenes) above 0.9% R_{max}, i.e., beyond the "second coalification jump" of Teichmüller (*1*). Thus, petrographically-recognizable physical transformations are shown to correspond to a major chemical restructuring of the vitrinite. Increases in rank also correspond to systematic variations in the distributions of the isomers of various polyaromatic compounds in the flash pyrolyzates, which can be exploited in the creation of indicators covering a wide range of thermal maturation.

Most attempts to generalize the molecular structure of bituminous coal have relied upon the concepts of clusters, that is, sub-units with a small number of fused aromatic ring systems connected by short aliphatic chains and heteroatom bridges (*e.g., 2*). The sub-units are conceived as "average" or "representative" of the larger coal structure and are convenient, as they can be represented graphically in two dimensions on a printed page. Such models are the results of synthesis of data from multiple sources, including elemental analysis, chromatographic and mass spectrometric evaluation of pyrolysis and chemolysis products, and spectroscopic studies, in particular solid state nuclear magnetic resonance (NMR) and infra-red (IR). These concepts can be extended using computerized three-dimensional modeling, which reveals likely interactions between the hypothetical sub-units, permitting the determination of the most energetically-favorable conformations (*3*). Through such efforts, there has been a recognition of the role of non-covalent bonding in the formation and stabilization of the 3-D structure, with hydrogen bonding important when functional groups containing oxygen are present and van der Waals forces serving to bind stacked adjacent aromatic ring structures (*3, 4*). However, in spite of their sophistication, such models suffer from an obvious deficiency in that they attempt to present a structure for whole coal, which is in fact a variable mixture of solid macerals of diverse biological origin, hence of differing

molecular structures from the outset (*5*), plus a complex mobile phase (*6, 7*). Flash pyrolysis studies of a variety of macerals isolated from the same coal or kerogen sample have shown that there are significant chemical differences among such macerals (*8-13*). In addition, the profound effects of increasing coal rank on chemical structure are not often included in molecular modeling attempts. Each maceral may be expected to react differently to thermal alteration, just as different organic matter types follow distinct pathways on van Krevelen diagrams (*14*). Recent studies have focused on the transition from lignin to fossil wood (vitrinite) of high volatile bituminous rank, thus following the evolution of a single maceral type through the early stages of coalification (*5, 15, 16*), using the lignin structure as the starting point for the development of a model of vitrinite.

The application of the medical technique of density gradient centrifugation (DGC) to sedimentary organic matter (*17*) permits the preparation of maceral concentrates in quantities suitable for chemical analysis. DGC is particularly effective in isolating vitrinite from humic coal (Bensley, D. F.; Crelling, J. C., *Fuel*, in press). The Upper Carboniferous Lower Kittanning seam of Pennsylvania and Ohio (USA) is a single coal bed, which if followed laterally, ranges in rank from sub-bituminous to low volatile bituminous (*18*). It thus provides an ideal rank series to monitor the effects of thermal alteration over the entire oil generation window. By examining pyrolyzates of high purity vitrinite concentrates from Kittanning samples, it should be possible to isolate the effects of increasing coal rank on the molecular structure of a single maceral type. This work is thus, in part, an extension of previous studies (*5*) into a higher rank range.

Experimental Methods

Vitrinite concentrates were prepared using four coals of different rank from the Lower Kittanning seam, obtained from the Pennsylvania State University sample bank (Table I). The coals were processed by mechanical crushing to <75 μm, and (after pre-treatment with liquid nitrogen to induce fracturing) by micronization using a fluid energy mill employing nitrogen carrier gas and a 3 mL/min. charge rate. Overall density properties of the samples were determined by density gradient centrifugation (DGC) of 2 g of micronized coal over a density range of 1.0 to 1.6 g/mL, in an aqueous solution of CsCl, the concentration of which varied systematically (*17*). Once the density ranges of the vitrinite group macerals were determined (Table I), fresh aliquots of the micronized samples were successively centrifuged in CsCl solutions of constant density corresponding to the lower and upper limits of the vitrinite range. These pre-concentrated vitrinites were subjected to a final centrifugation step over the appropriately narrow density range and individual vitrinite fractions were produced. Extreme care was taken to avoid any chance of multi-maceral or non-vitrinite maceral contamination. Semifusinite contamination was evaluated by monitoring reflectance distributions. Blue-light analysis showed no trace of fluorescence in the vitrinite fractions, indicating that there was no liptinite contamination. The purity of the vitrinite fractions was petrographically determined to be >99%. Reflectance data was obtained using a Leitz MPVIII compact microscope modified for rotational polarization reflectance (*19, 20*). It should be noted that for each sample, a wide range of reflectances was apparent, after each vitrinite fraction was examined individually. This phenomenon is discussed in detail elsewhere (Bensley, D. F.; Crelling, J. C., *Fuel*, in press).

For each of the four samples, an aliquot of the fraction corresponding to the approximate mode of the vitrinite DGC peak (Table I), pre-extracted with CH_2Cl_2, was subjected to analytical pyrolysis-gas chromatography/mass spectrometry (py-GC/MS). Pyrolysis was at 610° C for 20 sec., using a CDS 120 Pyroprobe coupled to an HP 5890A GC and an HP 5970B Mass Selective Detector. The pyrolysis temperature was monitored by a thermocouple situated inside the sample holder. The GC was equipped with a 25 m OV-1 column (0.2 mm i.d., 0.33 μm film thickness), initially held at 0° C for 5 min., then raised to

300° at 5°/min., then held for 15 min. The mass spectrometer was in full scan mode with an ionizing voltage of 70 eV.

Table I. Samples Employed and Their Reflectance and Density Values.

Sample (PSU)[a]	Sample (SIU)[b]	Bulk R_{max} (%)[c]	Vitrinite Density Range (g/mL)	Density Fraction Used (g/mL)	Fraction R_{max} (%)
PSOC-1289	SIU-1904	0.67	1.27-1.33	1.30	0.66
PSOC-1142	SIU-1889	0.81	1.25-1.31	1.30	0.82
PSOC-1145	SIU-1891	1.14	1.25-1.32	1.30	1.02
PSOC-1325	SIU-1907	1.59	1.24-1.29	1.27	1.39

[a]The Pennsylvania State University coal sample bank number.
[b]Coal sample number assigned at Southern Illinois University.
[c]Average vitrinite reflectance, measured at SIU on the whole coal sample.

Quantitations of the aromatic compounds of interest were performed on the Hewlett Packard data system, using the mass chromatograms of their molecular ions. All ratios used as indicators of the degree of thermal alteration are arranged such that the thermally stable components are in the numerator and the sum of the stable and labile are in the denominator. Thus all ratios increase with rank and are constrained to vary between 0 and 1. The exception is the Methylphenanthrene Index (*21*), which is used in its published form. Note that the plural forms of aromatic compound names are used to collectively refer to the principal compound and all detected pseudohomologues. For example, the group term "naphthalenes" is used to mean naphthalene plus the C_1 to C_3-alkylnaphthalenes. Compounds are also collectively designated herein by upper case Greek letters followed by an Arabic numeral, signifying the compound type(s) and the extent of methyl substitution (Figure 1). For example, "N_3" refers to C_3-alkylnaphthalenes and "Ψ_2" refers to compounds with a molecular ion of m/z 206, i.e., C_2-alkylphenanthrenes and C_2-alkylanthracenes.

Results and Discussion

Distributions of Aromatic Compounds by Class. The four vitrinite pyrolyzates all show a predominance of aromatic hydrocarbons and/or phenolic compounds. There are only minor amounts of aliphatic hydrocarbons, due to the absence of liptinites and extractable organic material. Phenol and C_1 to C_3-alkylphenols are the most abundant compounds for the 0.66% R_{max} vitrinite (Figures 1a and 2). In both relative and absolute terms, concentrations of the phenols diminish with increasing rank and thus, at 1.39% R_{max} they are only of minor importance (Figures 1b and 2), a phenomenon previously noted (*22, 23*). Naphthol, another aromatic alcohol, is also detectable as a significant compound in the 0.66% R_{max} pyrolyzate (Figure 1a), but not in the higher rank samples. The presence of hydroxyl functions in low rank vitrinites and their subsequent loss due to thermal alteration fits the well-documented decrease in the O/C atomic ratio for Type III organic matter as rank increases (*14*). It is the continuation of the trend of the loss of oxygen functionalities observed in the transition from lignin to sub-bituminous coal (*5,15,16*).

Mono- and Diaromatic Hydrocarbons. Monoaromatic hydrocarbons (C_1 to C_3-alkylbenzenes in particular) are important compounds for all vitrinite samples, regardless of rank (Peaks B_1-B_3 in Figure 1). Concentrations of monoaromatic hydrocarbons relative to other aromatics exhibit a minor decrease with rank (Figure 2). Benzene is detectable as a minor peak in all four pyrolyzates, but its low concentrations are in part an artifact of the

analytical conditions employed. Therefore, it should be noted that Figure 2 presents the quantitation results for unsubstituted plus monomethyl aromatic compounds, except in the case of the benzene series, for which methyl- plus dimethylbenzenes are used. Diaromatic hydrocarbons (naphthalene and C_1 to C_3-alkylnaphthalenes) are important components in all the pyrolyzates, especially the methyl- and dimethylnaphthalenes (Peaks N_1 and N_2 in Figure 1). Slightly higher relative concentrations of naphthalene plus methylnaphthalenes are noted for the vitrinites in the mid-rank range (0.82 and 1.02% R_{max}, Figure 2).

Triaromatic hydrocarbons. Triaromatic hydrocarbons are minor, although readily detectable, constituents of the low rank vitrinite pyrolyzate, with methylphenanthrene and methylanthracene the most notable (Ψ_1 in Figure 1a). In contrast, desmethyl-, methyl- and dimethylphenanthrenes are the most important peaks on the total ion current trace of the high rank pyrolyzate (Figure 1b). Relative and absolute concentrations of phenanthrene plus methylphenanthrenes increase sharply with rank, especially between the 0.82 and 1.02% R_{max} samples (Figure 2). The concentrations of fluorenes, in particular methylfluorene, are also greatly enhanced at high rank (Peak Λ_1 in Figure 1b).

Tetraaromatic Hydrocarbons. Fluoranthene, pyrene, benzo[*a*]fluorene, chrysene, benzo[*a*]anthracene and methylated derivatives are detectable, albeit faintly, in the lower rank pyrolyzates. The higher rank samples present a radically different picture, in which the tetraaromatics are among the major components, chrysenes and benzo[*a*]fluorene in particular (Figure 1b). The relative and absolute concentrations of "Group Π" compounds, including pyrene, fluoranthene, methylpyrenes and benzo[*a*]fluorene (i.e., those having molecular ions of m/z 202 and 216) increase sharply between 0.82 and 1.02% R_{max}, much like the phenanthrenes (Figure 2). The "Group X" compounds (those with molecular ions at m/z 228 and 242: chrysene, benzo[*a*]anthracene and their methylated derivatives) behave in an analogous fashion (Figure 2). The "second coalification jump" as defined by Teichmüller (*1*), occurring at ≈0.90% R_{max}, marks petrographically-recognizable physical changes in coal and the end of the *peak* stage of hydrocarbon generation. This boundary is shown here to correspond to profound changes in chemical structure of vitrinite as well, as seen in the sharp "chemical divide" visible between the 0.82 and 1.02% R_{max} samples in Figure 2.

The py-GC/MS results provide details of the evolution of the molecular structure of vitrinite with rank, going beyond the simple "increasing degree of condensation" previously inferred from solid state NMR data (*e.g., 7, 24*). The tri- and tetraaromatic hydrocarbons clearly dominate the pyrolyzates of the higher rank samples. These data suggest that the predominance of the larger aromatic structures is the result of progressive condensation (accelerating beyond 0.90% R_{max}) of smaller units, mostly phenolic structures as they undergo reduction.

Distributions of Polyaromatic Hydrocarbon Isomers. Profound rank-induced changes have been demonstrated in distribution of the aromatic compounds by number of rings, extent of methyl and hydroxyl substitution, and ring configuration. It is also of interest to examine the samples for variations in the distributions of key isomers of polyaromatic hydrocarbons (*25, 26*). The isomer clusters of interest can be observed on mass chromatograms of the appropriate molecular ion. Peaks can be quantitated and ratios calculated which may conveniently mark the progress of increasing thermal alteration. Such an approach is most frequently used on aromatic fractions of petroleums and source rock extracts. It is also advantageous to be able to apply such methods to flash pyrolyzates (*27*).

Trimethylnaphthalenes. The effect of an increase in rank from 0.66 to 1.39% R_{max} on the distributions of trimethylnaphthalene isomers can be observed on m/z 170 mass chromatograms (Figure 3). The 1,3,7-, 1,3,6- and 2,3,6-trimethyl isomers (Peaks 1, 2 and 4) are clearly favored at high rank. These isomers have been recognized for their superior

thermal stability in natural and artificially-matured samples, and also in light of theoretical considerations (*28-30*). Thus, their usefulness as indicators of the extent of thermal alteration may be expanded to include flash pyrolyzates. If the summed quantitation results of the three peaks are placed in the numerator, and those of all five trimethylnaphthalene peaks are in the denominator, the resulting "TMN" ratio increases slowly from 0.66 to 0.82% R_{max}, then more rapidly thereafter (Figure 4).

Phenanthrenes and Anthracenes. Distributions of phenanthrene, anthracene and their methylated variants also change significantly with rank, as seen on m/z 178 and 192 mass chromatograms (Figure 3). By 1.39% R_{max}, relative amounts of anthracenes and 9- and 1-methylphenanthrenes (Peaks 7, 10, 11 and 12) have decreased sharply. Methylphenanthrene Index or "MPI" (*21*) values show little change at lower ranks but increase sharply between 0.82 and 1.02% R_{max}, as the above-mentioned chemical divide is crossed (Figure 4). Equivalent vitrinite reflectance values (R_c, *25*) computed from the MPI of these experiments do not correspond well with the measured reflectances, especially at the lower ranks. This may be due to the coelution of a methylanthracene with 1-methylphenanthrene in Peak 12, which would have the effect of suppressing the ratio.

The anthracenes in the pyrolyzates are present in relative concentrations well in excess of what would be expected for petroleums and rock extracts (even coal extracts) of comparable rank. Since their concentrations are clearly rank dependent (Figure 3), they may also be exploited in the creation of thermal alteration indicators, applicable to vitrinite pyrolyzates. A simple ratio ("PA") of phenanthrene to the sum of anthracene and phenanthrene (Peaks 6/(6+7)) increases linearly up to 1.02% R_{max}, beyond which it stabilizes (Figure 4). This discontinuous behavior marks the crossing of the chemical divide. The 2- and 3-methylphenanthrenes and methylanthracene (Peaks 8, 9 and 10) are related in a similar fashion using the ratio "MPA" (Figure 4), which also exhibits a decrease in slope above 1.02% R_{max}.

The dimethylphenanthrenes (m/z 206, Figure 3) exhibit marked augmentation of the 2,6- and 2,7-dimethyl isomers (Peaks 14 and 15) as the vitrinite reflectance increases from 0.66 to 1.39% R_{max}. The thermal stability of these peaks has been previously noted, both by empirical observation and on a theoretical basis (*25, 26, 31, 32*). There is a coincident decrease observed for the less stable 1,6-, 2,9- and 1,7-dimethyl isomers (Peaks 18 and 19). These phenomena can be exploited in the creation of the "DPH" ratio (Figure 4), which increases smoothly throughout the entire rank range. The dramatic loss of dimethylanthracene (Peak 16, Figure 3) with rank could also be used as the basis for a ratio which would work for vitrinite pyrolyzates.

Tetraaromatic Hydrocarbons. Among "Π_1" compounds, benzo[*a*]fluorene (Peak 21, Figure 3) demonstrates a superior thermal stability over the methylpyrene isomers (Peaks 23, 25 and 26) seen on the m/z 216 mass chromatograms. Unidentified Peaks 22 and 24, which are probably methylfluoranthenes or other configurations of benzofluorene, also show relative decreases with rank. The resulting "MPY" ratio (Figure 4) has a sharp increase in slope between 0.82 and 1.02% R_{max}, above which it stabilizes. This apparently reflects once again the transition across the chemical divide. Closer examination of the m/z 216 mass chromatograms reveals that 2-methylpyrene (Peak 23) is favored over the other two methylpyrenes (Peaks 25 and 26) at high rank. This may be explained by the lesser steric hindrance at the C-2 position. An additional ratio could be created based on this phenomenon. Further rank effects are readily seen among the "Π_2" compounds (dimethylpyrenes and isomers) on m/z 230 traces.

The "X_0" tetraaromatic compounds also exhibit strong rank dependent effects (m/z 228, Figure 3). A sharp decrease in benzo[*a*]anthracene (Peak 27) concentrations relative to chrysene (Peak 28) is apparent. When the corresponding ratio ("CHR", Figure 4) is computed, the resulting curve shows a pronounced increase in slope between the 0.82 and

1.02% R_{max} vitrinites, as did the MPY ratio. Thus, the greatest loss of benzo[*a*]anthracene occurs during the transition corresponding to the chemical divide and the Teichmüller coalification jump (*1*). Distributions of the methylated variants of these compounds ("X_1"), as observed on m/z 242 mass chromatograms, are also significantly affected by the rank increase between 0.82 and 1.02% R_{max}.

Conclusions

Through the careful use of multi-step density gradient centrifugation, vitrinite concentrates of high purity were isolated from coal of the Lower Kittanning seam rank series. Chemical analyses of these concentrates permit one to focus on rank effects without concern for variations in organic matter type, over coal ranks corresponding to vitrinite reflectances ranging from 0.66 to 1.39% R_{max}, that is, the entire oil generation window.

In addition to the previously recognized losses of phenolic compounds with increasing rank, the vitrinite pyrolyzates exhibit marked increases in relative and absolute concentrations of tri- and tetraaromatic hydrocarbons, especially methylphenanthrene, methylfluorene, benzo[*a*]fluorene and methylchrysene isomers. There are only minor changes in the concentrations of mono- and diaromatic hydrocarbons — they are significant components at all rank levels examined. The 3- and 4-ring compounds are likely the products of the condensation of phenolic structures upon reduction.

The distributions of individual isomers of many of the polyaromatic hydrocarbons in the pyrolyzates also show pronounced rank effects. These phenomena may be exploited by the creation of ratios which respond to increases in the level of thermal alteration. Two such ratios are particularly effective over the full rank range studied. One depends on the thermal stability of the 1,3,7-, 1,3,6- and 2,3,6-trimethylnaphthalenes and the other, on the relatively robust 2,6- and 2,7-dimethylphenanthrenes. Other ratios exploit the thermal instability of anthracene and methylanthracene, compounds readily detectable in the pyrolyzates of low rank vitrinite.

Two other thermal indicator ratios computed for the pyrolyzates show sharp increases between the 0.82 and 1.02% R_{max} vitrinites. These ratios are based upon the superior stability of chrysene over benzo[*a*]anthracene and of benzo[*a*]fluorene over methylpyrenes. This is coincident with the sudden overall increase in tri- and tetraaromatic hydrocarbon concentrations. This "chemical divide" occurs at the same rank level as the second coalification jump of Teichmüller (*1*). Thus, petrographically-recognizable physical transformations in coal are shown be coincident with major chemical restructuring of the vitrinite.

Vitrinite has long been employed petrographically as a rank indicator. It now appears that its usefulness may be extended into the chemical realm, particularly through the use of flash pyrolysis. The isolation of high purity vitrinite concentrates permits analysis with the least possible interference by other organic matter types. However, as a practical matter, pyrolysis of organic matter samples with naturally high concentrations of vitrinite should also produce suitable results.

Literature Cited

1. Teichmüller, M. *Org. Geochem.* **1986**, *10*, 581-599.
2. Shinn, J. H. *Fuel* **1984**, *63*, 1187-1196.
3. Carlson, G. A. *Energy & Fuels* **1992**, *6*, 771-778.
4. Nishioka, M.; Larsen, J. W. *Energy & Fuels* **1990**, *4*, 100-106.
5. Hatcher, P. G.; Faulon, J.-L.; Wenzel, K. A.; Cody, G. D. *Energy & Fuels* **1992**, *6*, 813-820.
6. Given, P. H.; Marzec, A. *Fuel* **1988**, *67*, 242-244.
7. Haenel, M. W. *Fuel* **1992**, *71*, 1211-1223.

8. Nip, M.; de Leeuw, J.W.; Schenk, P.A. *Geochim. Cosmochim. Acta* **1988**, *52*, 637-648.
9. Nip, M.; de Leeuw, J.W.; Schenk, P.A.; Windig, W.; Meuzelaar, H.L.C.; Crelling, J.C. *Geochim. Cosmochim. Acta* **1989**, *53*, 671-683.
10. Giuliani, J. D.; Wang, P.; Dyrkacz, G. R.; Johns, R. B. *J. Anal. Applied Pyrolysis* **1991**, 20, 151-159.
11. Nip, M.; de Leeuw, J.W.; Crelling, J.C. *Energy & Fuels* **1992**, *6*, 125-136.
12. Stankiewicz, B. A.; Kruge, M. A.; Crelling, J. C. In *Programme et Recueil des Résumés, IXe Colloque International des Pétrographes Organiciens Francophones, 16-18 Juin 1993*; Elf Aquitaine Production: Pau, France.
13. Kruge , M. A.; Stankiewicz, B. A.; Crelling, J. C. In *Organic Geochemistry: Poster Sessions from the 16th International Meeting on Organic Geochemistry, Stavanger, 1993*; Øygard, K., Ed.; Falch Hurtigtrykk: Oslo, Norway, 1993; pp. 140-144.
14. Tissot, B. P.; Welte, D. H. *Petroleum Formation and Occurrence*; Springer-Verlag: Berlin, 1984; pp. 151-158 and 234-241.
15. Hatcher, P. G.; Lerch, H. E.; Bates, A. L.; Verheyen, T. V. *Org. Geochem.* **1989**, *14*, 145-155.
16. Hatcher, P. G. *Org. Geochem.* **1990**, *16*, 959-968.
17. Crelling, J.C. *Am. Chem. Soc. Div. Fuel Chem. Prepr.* **1989**, *34 (1)*, 249-255.
18. Hower, J. C.; Davis, A. *Geol. Soc. Am. Bull.* **1981**, 92, 350-366.
19. Houseknecht, D. W.; Bensley, D. F.; Hathon, L. A.; Kastens, L. A. *Org. Geochem.* **1993**, 20, 187-196.
20. Bensley, D. F.; Crelling, J. C. *Proceedings of the Int. Conf. on Coal Science*, 1993, Vol. 1, pp. 578-581.
21. Radke, M.; Welte, D.H. In *Advances in Organic Geochemistry 1981*; Bjøroy M. et al., Eds.; John Wiley & Sons, Ltd.: Chichester, 1983; pp. 504-512.
22. Sentfle, J. T.; Larter, S. R.; Bromley, B. W.; Brown, J. H. *Org. Geochem.* **1986**, 9, 345-350.
23. Venkatesan, M. I.; Ohta, K.; Stout, S. A.; Steinberg, S.; Oudin, J. L. *Org. Geochem.* **1993**, 20, 463-473.
24. Solum, M. S.; Pugmire, R. J.; Grant, D. M. *Energy & Fuels* **1989**, *3*, 187-193.
25. Radke, M. In *Advances in Petroleum Chemistry, Vol. 2*; Brooks J.; Welte D. H., Eds.; Academic Press: London, 1987, pp. 141-207.
26. Kruge, M. A.; Landais, P. *Preprints of Papers Presented at the 204th ACS National Meeting*; Amer. Chem. Soc. Div. of Fuel Chemistry: Washington, DC, 1992, Vol. 37, No. 4, pp. 1595-1600.
27. Requejo, A. G.; Gray, N. R.; Freund, H.; Thomann, H.; Melchior, M. T.; Gebhard, L. A.; Bernardo, M.; Pictroski, C. F.; Hsu, C. S. *Energy & Fuels* **1992**, *6*, 203-214.
28. Alexander, R.; Kagi, R.I.; Rowland, S.J.; Sheppard, P.N.; Chirila, T.V. *Geochim. Cosmochim. Acta* **1985**, *49*, 385-395.
29. Radke, M.; Welte, D.H.; Willsch, H. *Org. Geochem.* **1986**, *10*, 51-63.
30. Budzinski, H.; Garrigues, P.; Radke, M.; Connan, J.; Rayez, J. C.; Rayez, M. T. *Energy & Fuels* **1993**, *7*, 505-511.
31. Garrigues, P.; Oudin, J.L.; Parlanti, E.; Monin, J.C.; Robcis, S.; Bellocq, J. *Org. Geochem.* **1990**, *16*, 167-173.
32. Budzinski, H.; Garrigues, P.; Radke, M.; Connan, J.; Oudin, J. L. *Org. Geochem.* **1993**, *20*, 917-926.

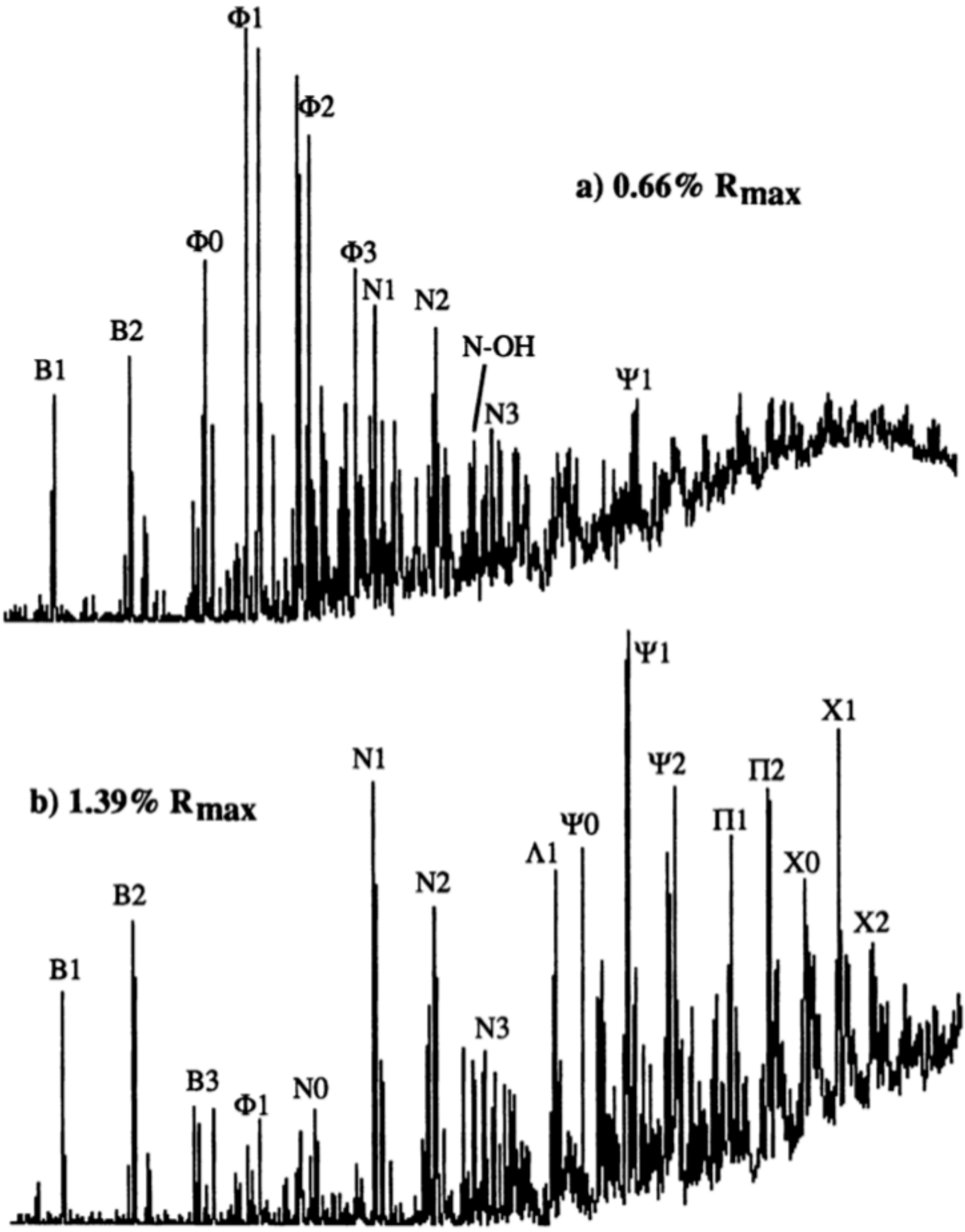

Vitrinite Pyrolyzates — Total Ion Current

Bn — Benzenes	Λn — Fluorenes
Φn — Phenols	Ψn — Phenanthrenes & Anthracenes
Nn — Naphthalenes	Πn — Pyrenes, Fluoranthenes and Benzo[*a*]fluorene
N-OH — Naphthol	Xn — Chrysenes and Benzo[*a*]anthracene

where "n" indicates extent of methyl substitution

Figure 1 — Py-GC/MS total ion current chromatograms of solvent-extracted vitrinite concentrates. a) Low rank example. b) High rank example.

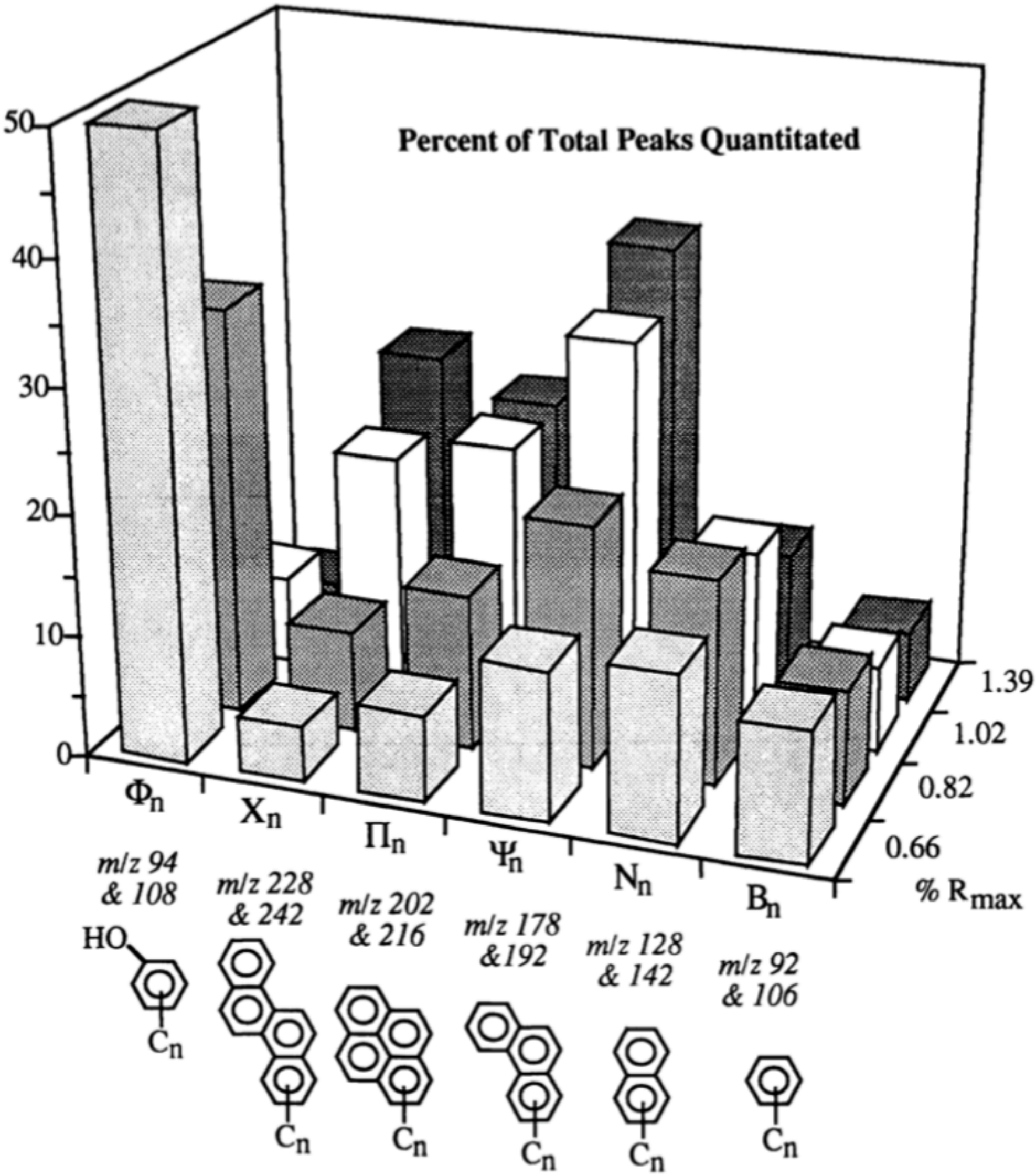

Figure 2. Relative quantitation results for key aromatic and phenolic compounds in the flash pyrolyzates of four vitrinite concentrates. Compound groups are designated by upper case Greek letters as in Figure 1. Molecular ions used in quantitation are given. Examples of molecular structures are also shown, but it should be noted that "Group X" also includes benzo[a]anthracene, "Group Π" also includes fluoranthene and benzo[a]fluorene, and "Group Ψ" also includes anthracene. Subscript "n" indicates the extent of methyl substitution (n = 0 and 1 for all compounds except the benzene series, for which n = 1 and 2). See text for further explanation.

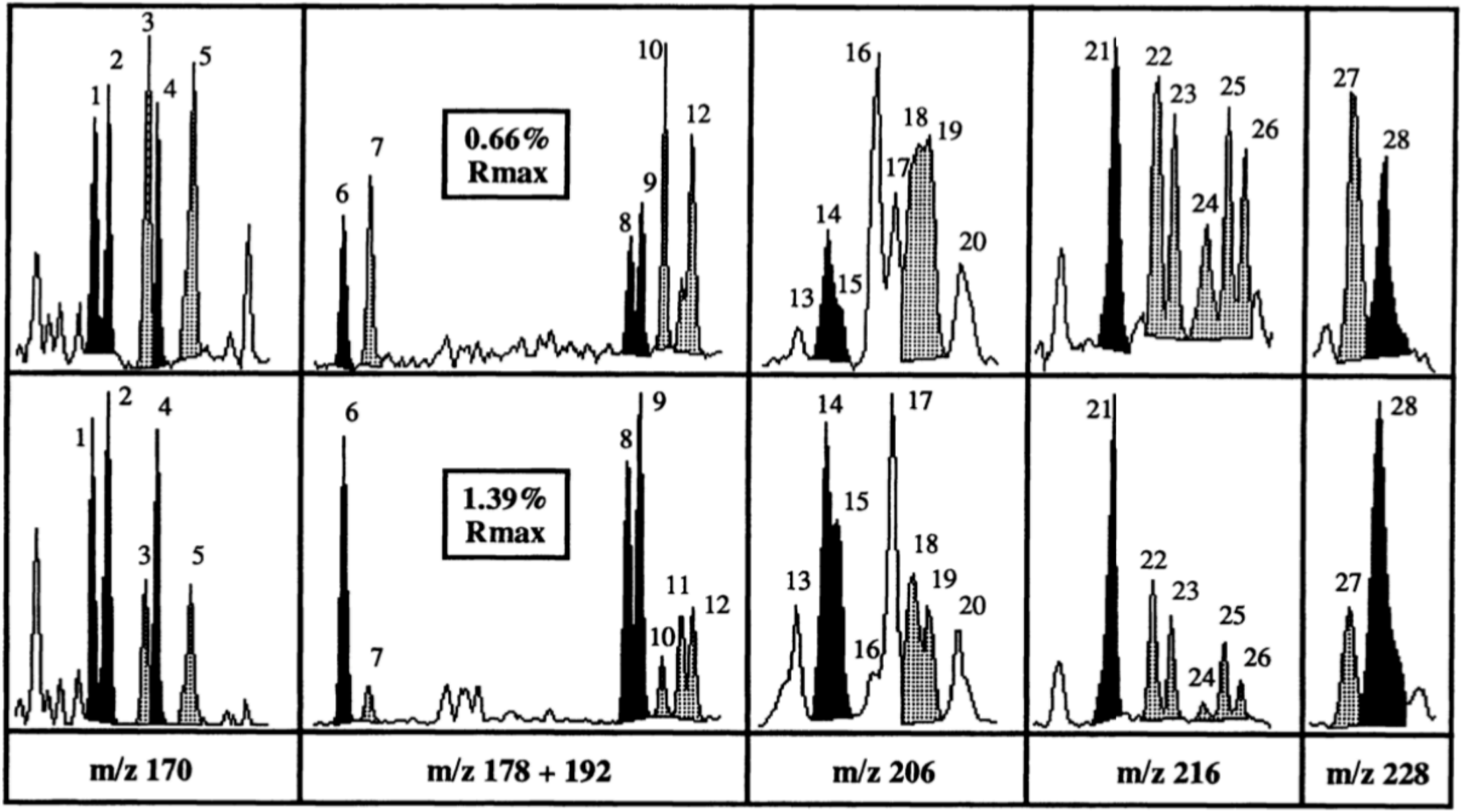

Figure 3. Mass chromatograms of selected polyaromatic isomer groups for low rank (top row) and high rank (bottom row) vitrinite concentrates. Compounds are identified in Table II. Peaks used in the thermal alteration indicator ratios of Figure 4 are shown in black if they are thermally stable and stippled if they are labile. See text for further explanation.

Table II — Identification of Peaks Used in Figure 3.

Peak	m/z	Group[a]	Compound(s)
1	170	N_3	1,3,7-trimethylnaphthalene
2	170	N_3	1,3,6-trimethylnaphthalene
3	170	N_3	1,4,6- & 1,3,5-trimethylnaphthalenes
4	170	N_3	2,3,6-trimethylnaphthalene
5	170	N_3	1,2,7- & 1,6,7- & 1,2,6-trimethylnaphthalenes
6	178	Ψ_0	phenanthrene
7	178	Ψ_0	anthracene
8	192	Ψ_1	3-methylphenanthrene
9	192	Ψ_1	2-methylphenanthrene
10	192	Ψ_1	methylanthracene
11	192	Ψ_1	9-methylphenanthrene
12	192	Ψ_1	1-methylphenanthrene & methylanthracene
13	206	Ψ_2	3,6-dimethylphenanthrene
14	206	Ψ_2	2,6-dimethylphenanthrene
15	206	Ψ_2	2,7-dimethylphenanthrene
16	206	Ψ_2	dimethylanthracene
17	206	Ψ_2	1,3- & 2,10- & 3,9- & 3,10-dimethylphenanthrenes
18	206	Ψ_2	1,6- & 2,9-dimethylphenanthrenes
19	206	Ψ_2	1,7-dimethylphenanthrene
20	206	Ψ_2	2,3- & 1,9- & 4,9-dimethylphenanthrenes
21	216	Π_1	benzo[*a*]fluorene
22	216	Π_1	methylfluoranthene or benzofluorene (?)
23	216	Π_1	2-methylpyrene
24	216	Π_1	methylfluoranthene or benzofluorene (?)
25	216	Π_1	4-methylpyrene
26	216	Π_1	1-methylpyrene
27	228	X_0	benzo[*a*]anthracene
28	228	X_0	chrysene

[a]For comparison with total ion chromatograms in Figure 1.

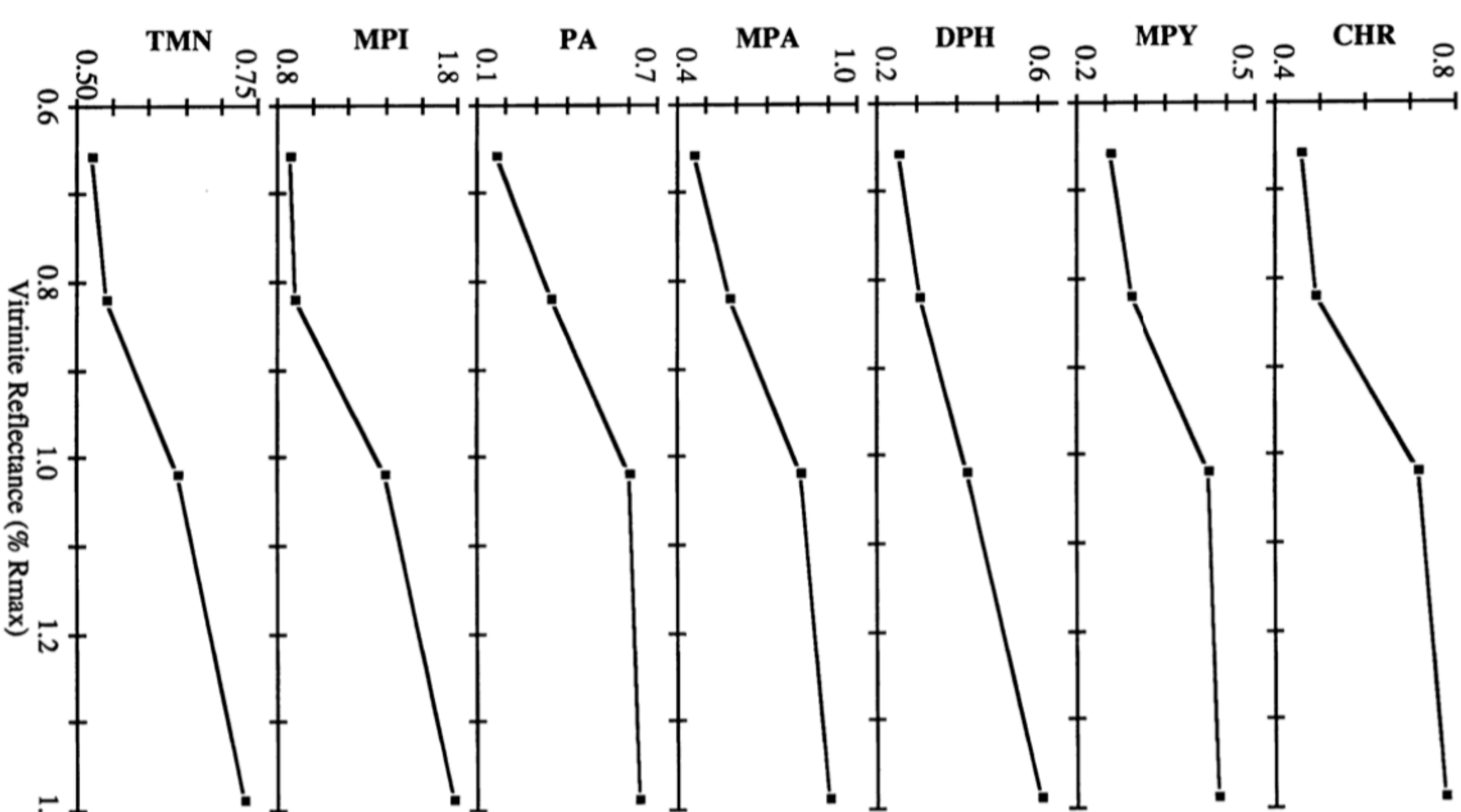

Figure 4. Thermal alteration indicator ratios. Peaks employed in the ratios and the MS ions used in their quantitation are identified in Table I. *TMN*: Peaks (1+2+4) / (1+2+3+4+5). *MPI*: (1.5 (Peaks 8+9) / (Peaks 6+11+12). *PA*: Peaks 6 / (6+7). *MPA*: Peaks (8+9) / (8+9+10). *DPH*: Peaks (14+15) / (14+15+18+19). *MPY*: Peaks 21 / (21+22+23+24+25+26). *CHR*: Peaks 28 / (27+28). See text for further explanation.